Accepted Manuscript
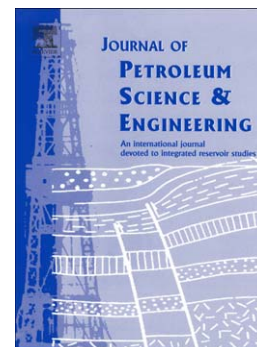
Estimation of the fracture density in fractured zones using petrophysical logs

Behzad Tokhmchi, Hossein Memarian, M. Reza Rezaee

Please cite this article as: Tokhmchi, Behzad, Memarian, Hossein, Rezaee, M. Reza, Estimation of the fracture density in fractured zones using petrophysical logs, *Journal of Petroleum Science and Engineering* (2010), doi: 10.1016/j.petrol.2010.03.018

Estimation of the fracture density in fractured zones using petrophysical logs

Behzad Tokhmchi[a,b,*]**, Hossein Memarian**[b,c]**, M.Reza Rezaee**[d]

[a] School of Mining, Petroleum and Geophysics Engineering, Shahrood University of Technology,

Shahrood, Iran

[b] School of Mining Engineering, University of Tehran, Tehran, Iran
[c] Department of Earth & Environmental Sciences, University of Waterloo, Ontario, Canada
[d] Department of Petroleum Engineering, Curtin University of Technology, Perth, Australia

Abstract

Image logs are presently the main specialized tools for fracture detection in hydrocarbon reservoirs. Where image logs are not available, other less rewarding substitutes such as isolated well tests and type curve analysis, drilling mud loss history, core description and conventional petrophysical logs are used for fracture detection. In this paper a novel method is proposed for fracture density estimation in the fractured zones, using energy of petrophysical logs. Image and petrophysical logs from Asmari reservoir in eight wells of an oilfield in southwestern Iran were used to investigate the accuracy and applicability of the proposed method. Energy of the petrophysical logs in the fractured zones is calculated and linear and non-linear regressions between them are estimated. Results show that there is strong correlation between the energy of caliper, sonic (DT), density (RHOB) and lithology (PEF) logs with fracture density in each well. In order to find a generalized estimator, a unique normalization method are developed, and by using it, a non-linear regression has been found which estimates fracture density with correlation coefficient of higher than 80%. The resultant regression has the capability of generalization in the studied field.

1. Introduction

Natural fractures have significant influence on the reservoir behavior and performance. Therefore, in modeling fractured reservoirs, understanding fracture properties is very important (Roehl and Choquette 1985). Fractured zones can be probably detected both directly and indirectly using seismic sections, petrophysical logs, well tests, drilling mud loss history and core description (Thompson 2000, Nelson 2001, Martinez-Torres 2002, Dutta *et al* 2007, Tokhmechi *et al* 2009a, b). However, each of these methods is subjected to some limitations in practice.

Since mid 1980's, and introduction of dipmeter technology and image logs, the process of fracture detection and characterization of fracture properties; such as dip, dip direction, fracture density and opening; has become less problematic (Serra 1989). Presently, these high resolution data acquisition devices can detect small scale variations and discontinuities in rocks. Unfortunately, no image log is available for thousands of wells drilled before introduction of these new technologies.

As fractures modeling with an inadequate volume of data can lead to misleading interpretations, any direct or indirect techniques which increase the knowledge of fracture properties is highly valuable. In general, fracture modeling is an object based practice which

---

* Corresponding author at: Assistant Professor, School of Mining, Petroleum and Geophysics Engineering, Shahrood University of Technology, Haft Tir Boulevard, Shahrood, Iran, Tel: +98-21-88634224; Fax: +98-21-88637621; Email address: *tokhmechi@ut.ac.ir*

 memarian@ut.ac.ir (H. Memarian), r.rezaee@curtin.edu.au (M. R. Rezaee)

requires a larger amount of data, compare to pixel based modeling, because of dividing data in some object sets in object based modeling, which each set is separately used in modeling.

Earlier attempts to detect natural fractures include the use of sonic waves (Hsu 1987), wavelet transform (Daiguii *et al* 1997), a so called velocity deviation log (Flavio and Gregor 1999), core data (Song *et al* 1998) and seismic data (Behrens *et al* 1998). In a recent attempt, wavelet transform was applied on porosity log data and it was suggested that high frequency variations correspond to the existence of fractures (Sahimi and Hashemi 2001). To validate the model, permeability data were used, where large increases in permeability correspond to the existence of fractures. Surjaatmadja *et al* (2002) used a frequency decomposition approach to analyze downhole data to detect natural fractures. Martinez-Torres (2002) applied a fuzzy logic technique to various petrophysical logs, while a classification algorithm was used by Tran (2004) to study and detect natural fractures. Shen and Li (2004) have presented a combined approach for characterization of naturally fractured reservoirs. Application of shear-wave technique to identify fault zones (Dutta *et al* 2007), a wavelet transform applied to petrophysical logs (Mohebbi *et al* 2007), factor analysis to detect open fractures near faults (Ozkaya and Siyabi 2008) and detecting fracture corridors using probabilistic decision trees (Ozkaya 2008) are other methods used by other researchers to identify and characterize natural fractures. Yan *et al* (2009) presented a method to model fracture porosity. They used petrophysical logs in order to create a synthetic image log. Proposed method was checked in a well of a gas saturated carbonate reservoir. This study revealed that it is possible to identify fractures location and some of their properties. Tokhmechi *et al* (2009a and b) developed novel approaches in order to detect fractured zones using petrophysical logs. They have used wavelet, classification and data fusion techniques in their approaches. They have checked the generalization of proposed methods in eight wells in one of the giant carbonated oil fields of south western Iran. The validation of methods has been checked with image logs. It seems that methods proposed in these two papers have good validation and capability for fractured zone detection.

Except the last two mentioned papers, the main deficiency of the majority of the previous studies are inadequate volumes of data and failing to validate the method due to lack of image logs. More importantly, it is impractical to evaluate generalization possibility in the results, even to nearby wells, where the data are inadequate.

In this paper a new method has been presented to estimate fracture density in fractured zones. All available conventional petrophysical logs have been used in proposed methodology. Simple linear and non-linear estimators have been used in order to develop an equation with high generalization capability. The proposed methodology has been applied to eight vertical wells in an oilfield located in the southwest Iran, where sequences of fractured zones with variable fracture density is observed along with non-fractured intervals in the Oligo-Miocene Asmari carbonate Formation (Alavi 2004). UGC map of the top of Asmari of studied oilfield and locations and the number of studied wells in oilfield are shown in figure 1. As it can be seen in figure 1 existence of some faults in studied area and variation in formation curvature introduced some heterogeneity in respect to fracture distribution. A large volume of data has been used in this analyzes, which enables us not only to check the accuracy of the method, but also to study the possibility of its generalization.

Figure 1

2. Methods and materials
In this section, two techniques and data used in this study have been briefly presented.

2.1 Petrophysical logs energy
Calculation of petrophysical logs energy is a simple procedure that magnifies the differences between log data. The following procedure has been used to calculate petrophysical log energy for each log:
a. Select suitable logs for each well,

b. Identify fractured zones in each well using petrophysical logs and the approaches proposed by Tokhmechi *et al* (2009a and b),

c. Calculate petrophysical log energy (E_{PL}) for each fractured zone using Equation (1):

$$E_{PL} = \sum_{i=1}^{n} PL_i^2 \tag{1}$$

where *PL* and *n* are the amount of petrophysical log and the number of petrophysical log in each fractured zone respectively.

d. Assign the result of part *c* for each fractured zone.

In the end of the procedure a new log is created which the number of its members is equal to the number of fractured zones in studied well. This log is named energy log in this paper.

2.2 Normalization of the energy logs
Normalization of energy log follows the following algorithm:

a. Calculate mean of energy log in each well:

$$ME_{PL} = \frac{\displaystyle\sum_{j=1}^{C} E_{PL_j} . n_j}{\displaystyle\sum_{j=1}^{C} n_j} \tag{2}$$

where ME_{PL} is the mean of energy log of certain petrophysical log in each well. E_{PL_j} and n_j are as the same as equation 1 in each fractured zone. C is the number of fractured zones in each well.

b. Calculate the mean of energy log (MZE_{PL_j}) in each zone:

$$MZE_{PL_j} = ME_{PL} . n_j \tag{3}$$

The amounts of MZE_{PL_j} depend on petrophysical logs, but their variation is independent of petrophysical logs. Therefore it is a unique normalization method because normalized numbers depends to fractured zones thickness and mean weighted values of various petrophysical logs in fractured zones.

2.3 Materials
More than 300 wells are drilled in the studied field. Whole suit of conventional logs including caliper, Density, Neutron, Sonic, resistivity and natural gamma ray spectrometry ran in most of them whereas image logs ran in only eight wells. There are some probabilistic methods that can help identifying fractured zones in the wells without image logs. As the studied reservoir is a naturally fractured formation, estimating fracture density in fractured zones using petrophysical logs helps generating valuable data for about 300 wells. Petrophysical logs and interpreted image logs of eight studied wells were used to generate an estimator of fracture density in fractured zones which can be generalized to all wells. Fractured zones and the number of fractures in each fractured zone (fracture density) are identified from interpretation of image logs.

3. Discussion
This approach will be useful if a generalized correlation between energy log and fracture density in each fractured zones can be established.

3.1 Correlation between energy log and fracture density
Good linear regression is observed between energy log of some of the petrophysical logs and fracture density in fractured zones of each well. For example, regressions in well #3 are shown in figure 2. As it can be seen in this figure, correlation coefficient for caliper, DT, RHOB and PEF are higher than 0.97. Therefore it is clear that estimation of fracture density in fractured zones using those petrophysical logs leads to accurate prediction of fracture

density. Correlation coefficients of linear regressions between energy log and fracture density in fractured zones of various wells are listed in table 1. Based on these results, except for well 4 which has lowest fractured zones, in the other wells correlation coefficient of caliper, DT, RHOB and PEF are higher than 0.7. Therefore, above named petrophysical logs were selected for generalization stage. The fracture density in each fractured zone and selected petrophysical logs of well #1 are shown in figure 3. In figure 4 image log of well #1 and corresponding fracture density in each fractured zone are shown. As it can be seen in these figures, there is no visible relation between fracture density and petrophysical logs in this well.

Figure 2

Table 1

Figure 3

Figure 4

Energy log data of selected petrophysical logs of eight studied wells are gathered together to investigate linear or non-linear regression between energy log and fracture density. The results are shown in figure 3. According to the results, no strong linear or nonlinear regression is observed. Only coefficient correlation of non-linear regression of caliper and PEF are higher than 0.63. Although these two correlations are not poor, but they are less than 0.7, indicating that estimation is not reliable. Therefore we should generate other regressions with better correlation.

3.2 Generating better generalized regressions

Figure 5 shows that in generalization stage, fitness of simple non-linear regression to data is better than linear regression. Therefore, a new generalized simple non-linear regression with higher correlation coefficient should be found. For this purpose, energy log data of all wells are accumulated and normalized using equations 2 and 3. As mentioned before, normalized data merely depend on the thickness of fractured zones and are independent of the type of petrophysical logs. Non-linear regression between normalized energy log (NEL) and fracture density in eight studied wells for four selected petrophysical logs is shown in figure 6. As it can be seen in this figure, the correlation coefficients of non-linear regressions are higher than 0.7 (i.e. 0.74) and independent from petrophysical logs. The figures of four non-linear regressions are similar, but their coefficients differ, because they just depend on the ME_{PL} (equation 2).

Figure 5

Figure 6

As it can be seen in figure 6, the parametric figure of non-linear regression equations show a general form of:

$$FD = a.NEL^b \tag{4}$$

where a and b are constant and depend on the mean of fracture density and mean of energy log in each zone. The simple way for definition a and b is converting an exponential curve to a linear one, using the following algorithm:

$$\log(FD) = \log(a.NEL^b) \quad \Rightarrow \quad \log(FD) = \log(a) + b\log(NEL) \tag{5}$$

This expresses that *log(fracture density)* is a linear function of *log(NEL),* where b is line slope and log(a) is intercept. Therefore, if we find the best fit line, using *log(fracture density)* as a function of *log(NEL), fracture density* can obtained.

Of course, there is another tentative way for defining *a* and *b*. Slope *a* is defined as follows:

$$a = \frac{MFD}{MEL \times 36.85} \qquad (7)$$

where MFD is the mean of fracture density in each fractured zone and MEL is the mean of energy log in the resolution thickness of petrophysical logs (0.1526 meter). The coefficient 36.85 is calculated using numerical optimization of estimation with the aim of minimizing error. Based on these parameters, calculation of coefficient *a* is very simple.

Power *b* just depends to MFD and it is independent of energy log. Therefore it is constant for various petrophysical logs. *b* can be calculated using following equation:

$$b = MFD \times 0.06 \qquad (8)$$

where 0.06 is a constant coefficient and independent from studied data. For example, as it can be seen in figure 6, *b* remains constant with changing the petrophysical logs. In figure 6, *b* approaches to one, which means non-linear regression approaches to a linear one.

It is clear that the error of estimation, which is the difference between the number of fractures in each fractured zone find in image log minus the estimated number of fractures; varies for various petrophysical logs. This is because slope *a* depends on the MEL. According to the results, sonic log (DT) is the best petrophysical log with the least error for fracture density estimation (figure 7). In this figure, error is increased with increasing the energy log corresponds with *increasing the thickness of fractured zones.*

Figure 7

Two trends are visible in figures 3 and 4. Fracture density of fractured zones of wells #1, 2 and 5 are underestimated, whereas in other wells we face overestimation. This has happened because of variation in fracture density. In table 2, fracture density of eight wells, as well as all wells and two separated groups of wells, in each unit thickness (0.1526 meter), are reported. As it can be seen in this table, based on fracture density, obviously two categories of wells exist. Fracture density per unit thickness, for group one and two are 0.67 and 0.31 respectively.

Table 2

Non-linear regression for two groups of wells, with high and low fracture density, is fitted separately. Results are presented in figure 8. The equations of figure 8 can be calculated using equations 4 to 8. Based on these figures, new non-linear regressions are better fitted to data, which means the error of estimation is decreased and coefficient correlations are increased to about 0.8. In figure 9 estimation error of fracture density for all wells are plotted, which shows the boundary of error is decreased to about half in comparison with figure 7. Therefore it can be concluded that fracture density estimation error will decrease if we can separate wells with high and low fracture density.

Figure 8

Figure 9

4. Conclusion

This paper proposes a novel method to estimate fracture density in fractured zones using petrophysical logs. High volume of the data used in this study is one of the points of strength which can support the validity of the results. Image logs of eight wells in an Iranian oil field were used in order to identify fractured zones and fracture density. Petrophysical logs of the wells are used for estimation of fracture density in fractured zones. Energy logs and NELs are calculated as the base data of estimation. In order to find better generalized estimator, NEL is calculated and non-linear regression is utilized. According to the results, if MFD in various wells strongly differs, the high and low MFD wells should be separated. In conclusion, the findings of this paper are:

- It is possible to fit linear regressions between energy log and fracture density in each well separately.
- For this purpose four petrophysical logs, caliper, sonic (DT), density (RHOB) and lithology (PEF), are more suitable.
- The arithmetic average correlation coefficient of linear regression between energy log and fracture density in eight studied wells for caliper and sonic logs is about 90%, which indicates existence of high correlation between them.
- A simple power regression is established which as an unbiased estimator approximate fracture density in fractured zones with about 0.74 correlation coefficient.
- The figure of this estimator is independent from utilized petrophysical log, and just its slope and intercept depend on the MFD and MEL.
- After separation of high and low MFD, the average correlation coefficient increased to about 0.80.

Abbreviations

DT sonic log
E_{PL} energy of petrophysical logs
MEL mean of energy log in the resolution thickness of petrophysical logs (0.1526 meter)
ME_{PL} mean of energy log of certain petrophysical log in each well
MFD mean of fracture density in each fractured zone
$MZE_{PL\,j}$ mean of energy log in each zone
NEL normalized energy log
PEF lithology log
$RHOB$ density log

References

Alavi, M., 2004. Regional stratigraphy of the Zagross fold-thrust belt of Iran and its proforeland evolution. AJS. 304, 1-20.

Behrens, R.A., Macleod, M.K., Tran, T.T., Alimi, A.O., 1998. Incorporating seismic attribute maps in 3D reservoir models. SPE Reserv. Evalu. 1, 122–126.

Daiguji, M., Kudo, O., Wada, T., 1997. Application of Wavelet Analysis to Fault Detection in Oil Refinery, Computers Chem Engng. 21, Suppl., S 1117-S 1122.

Dutta, P., Singh, S.K., Al-Genai, J., Akhtar, A., Akbar, M., 2007. A novel approach to fracture characterization utilizing borehole seismic data. 15th SPE Middle East Oil & Gas Show and Conference, Bahrain. Paper SPE 105427 (6 pp).

Flavio, S.A., Gregor, P.E., 1999. The velocity-deviation log A tool to predict pore type and permeability trends in carbonate drill holes from sonic and porosity or density logs. Am. Assoc. Pet. Geol. Bull. 83 (3), 450–466.

Hsu, K., Brie, A., Plumb, R.A., 1987. A new method for fracture identification using array sonic TOOIS. J. Pet. Technol. 677–683 June 1987, Paper SPE 14397.

Martinez-Torres, L.P., 2002. Characterization of Naturally Fractured Reservoirs from Conventional Well Logs. M.Sc. Thesis, University of Oklahoma. USA.

Mohebbi, A.R., Haghighi, M., Sahimi, M., 2007. Using conventional logs for fracture detection and characterization in one of Iranian field. International Petroleum Technology Conference held in Dubai, U.A.E., 4–6 December 2007, Paper IPTC 11186.

Nelson, R.A., 2001. Geologic Analysis of Naturally Fractured Reservoirs, SECOND EDITION. Gulf Professional Publishing, U.S.A. 332 pages.

Ozkaya, S.I., 2008. Using probabilistic decision trees to detect fracture corridors from dynamic data in mature oil fields. SPE Reserv. Evalu. 11 (6), 1061-1070.

Ozkaya, S.I., Siyabi, S., 2008. Detection of fracture corridors from dynamic data by factor analysis. SPE Saudi Arabia Section Technical Symposium held in Alkhobar, Paper SPE 120812.

Roehl, P.O., Choduette, P.W., 1985. Carbonate Petroleum Reservoirs. Spring-Verlag, New York. 622 pages.

Sahimi, M., Hashemi, M., 2001. Wavelet identification of the spatial distribution of fractures. Geophys. Reserv. Lett. 28 (4), 611–614.

Serra, O., 1989. Formation MicroScanner Image Interpretation, Schlumberger Education Services.

Shen, F., Li, S., 2004. A combined geological, geophysical and rock mechanics approach to naturally fractured reservoir characterization and its applications. SPE Annual Technique Conference and Exhibition, Houston. Paper SPE 90275 (8 pp).

Song, X., Zhu, Y., Iiu, Q., Chen, J., Ren, D., Li, Y., Wang, B., Liao, M., 1998. Identification and distribution of natural fractures. SPE International Conference and Exhibition in China held in Beijing, Paper SPE 50877.

Surjaatmadja, J.B., Stephenson, S., Cheng, A., 2002. Analysis of generated and reflected pressure waves during fracturing reveals fracture behavior. SPE Annual Technical Conf. and Exhibition held in San Antonio, Texas. Paper SPE 77598.

Thompson, L.B., 2000. Fractured reservoirs: integration is the key of optimization. Distinguished Author Series, 52–54, SPE 56010.

Tokhmechi, B., Memarian, H., Noubari, H.A., Moshiri, B., 2009a. A novel approach proposed for fractured zone detection using petrophysical logs. J. Geophys. Eng. Under publishing.

Tokhmechi, B., Memarian, H., Rasouli, V., Noubari, H.A., Moshiri, B., 2009b. Fracture detection from water saturation log data using a Fourier-Wavelet approach. J Petrol Sci Eng. Under publishing.

Tran, N.H., 2004. Characterization and Modeling of Naturally Fractured Reservoirs. Ph.D. Thesis, University of New South Wales, Australia.

Yan, J., Lu, L., Lubbe, R., Payne, S., 2009. Petrophysical fracture identification for rock physics studies. 71st EAGE Conf. & Exhibition, Amsterdam. (5 pp).

Table 1. Correlation coefficient of linear regression between energy log and fracture density in the fractured zones for eight studied wells.

Table 2. Mean of fracture density in unit thickness of eight studied wells as well as high and low density groups.

Figure 1. UGC map of oilfield and locations of the studied wells.

Figure 2. Linear regression between energy log and fracture density in the fractured zones for well #3.

Figure 3. The fracture density in each fractured zone and selected petrophysical logs for well #1.

Figure 4. Interpreted image log and fracture density in 30 meters of well #1.

Figure 5. Linear and non-linear regression between energy log and fracture density in fractured zones of eight studied wells. a) Caliper, b) DT, c) RHOB and d) PEF.

Figure 6. Non-linear regression between NEL and fracture density in fractured zones of eight studied wells

Figure 7. Error of estimation fracture density using sonic (DT) log and equation 4 in eight studied wells.

Figure 8. Non-linear regression between NEL and fracture density in fractured zones of two groups of wells with high (a) and low (b) fracture density

Figure 9. Error of estimation fracture density using sonic (DT) log and equations 4 to 8 in eight studied wells. Here the energy of petrophysical logs is normalized.
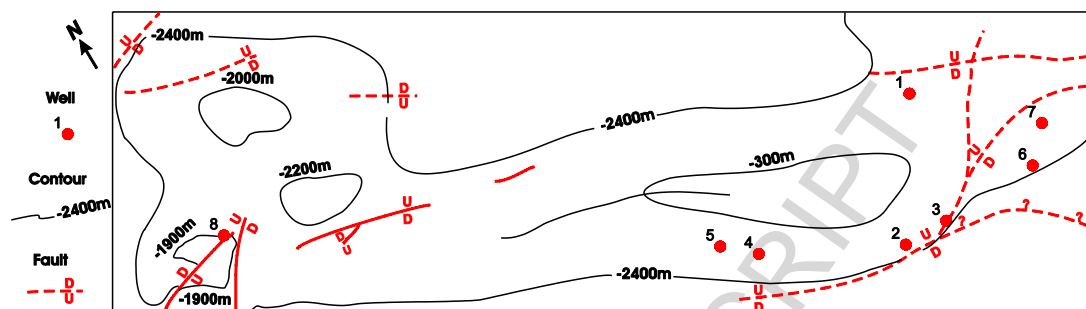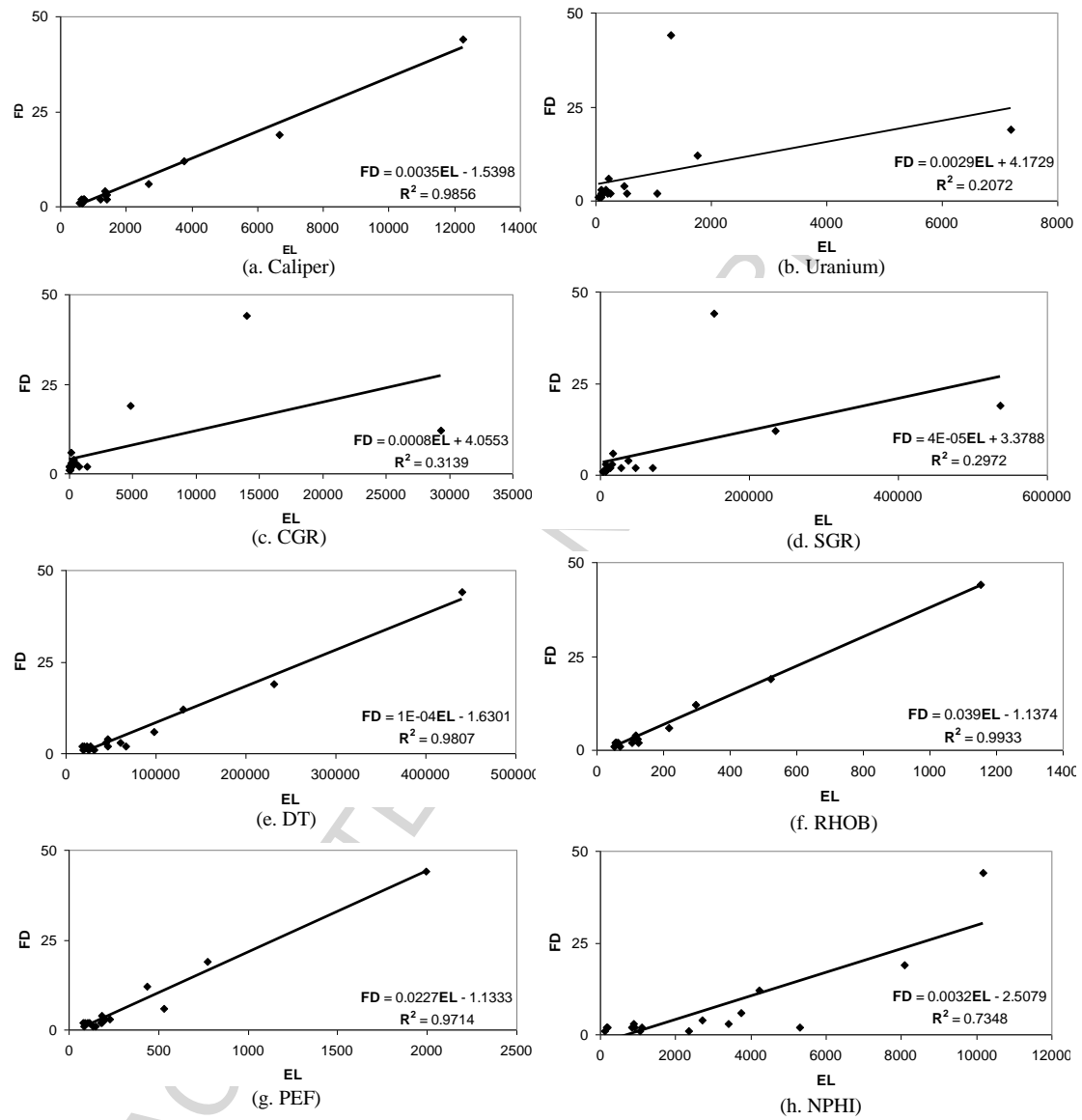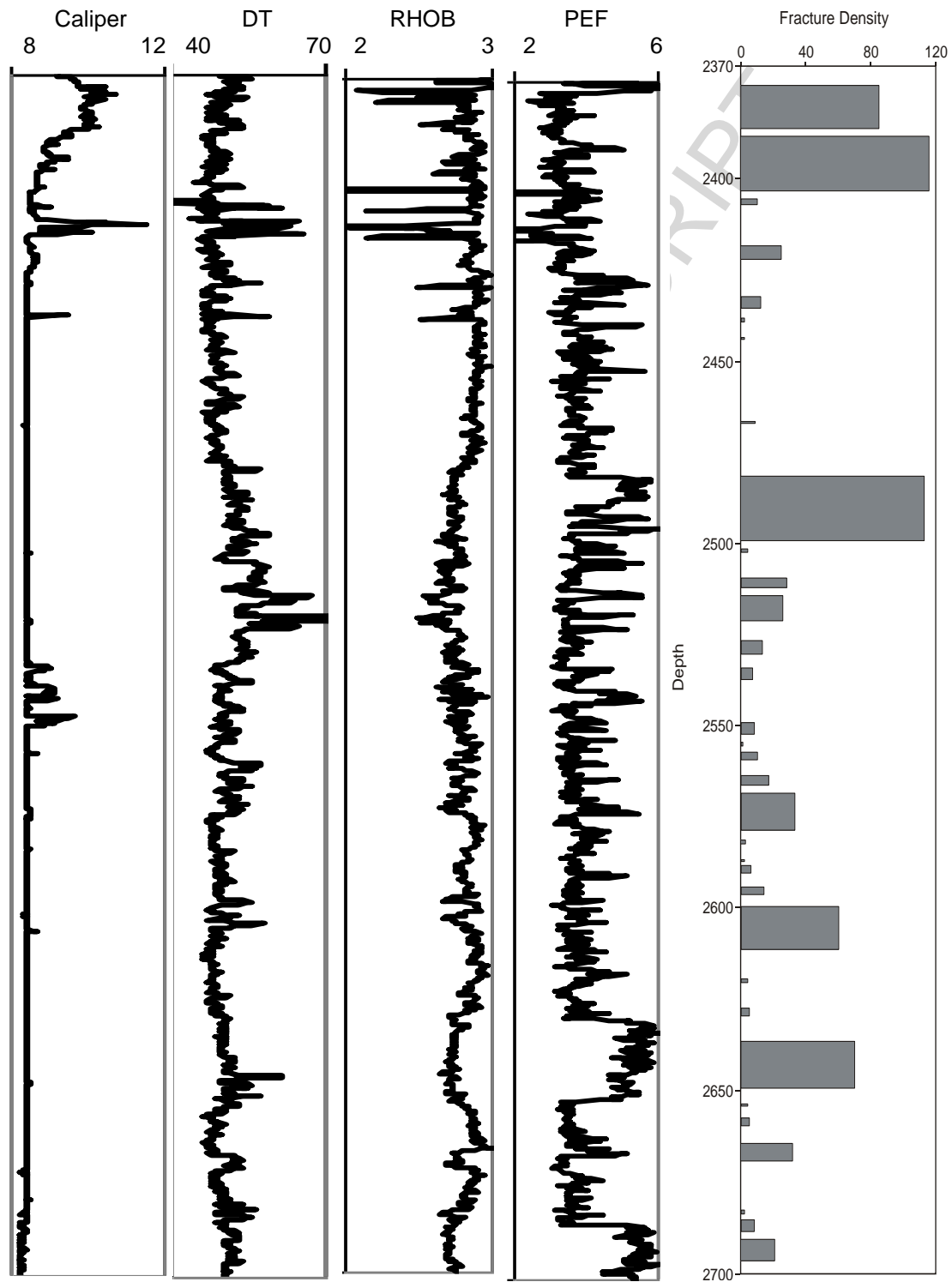
Fig. 1

Fig. 2

(a. Caliper)

FD = 0.0035**EL** - 1.5398
R^2 = 0.9856

(b. Uranium)

FD = 0.0029**EL** + 4.1729
R^2 = 0.2072

(c. CGR)

FD = 0.0008**EL** + 4.0553
R^2 = 0.3139

(d. SGR)

FD = 4E-05**EL** + 3.3788
R^2 = 0.2972

(e. DT)

FD = 1E-04**EL** - 1.6301
R^2 = 0.9807

(f. RHOB)

FD = 0.039**EL** - 1.1374
R^2 = 0.9933

(g. PEF)

FD = 0.0227**EL** - 1.1333
R^2 = 0.9714

(h. NPHI)

FD = 0.0032**EL** - 2.5079
R^2 = 0.7348

10

Fig. 3

Figure 3. The fracture density in each fractured zones and selected petrophysical logs for well #1.

11

Fig. 4

(a)

(b)

(c)

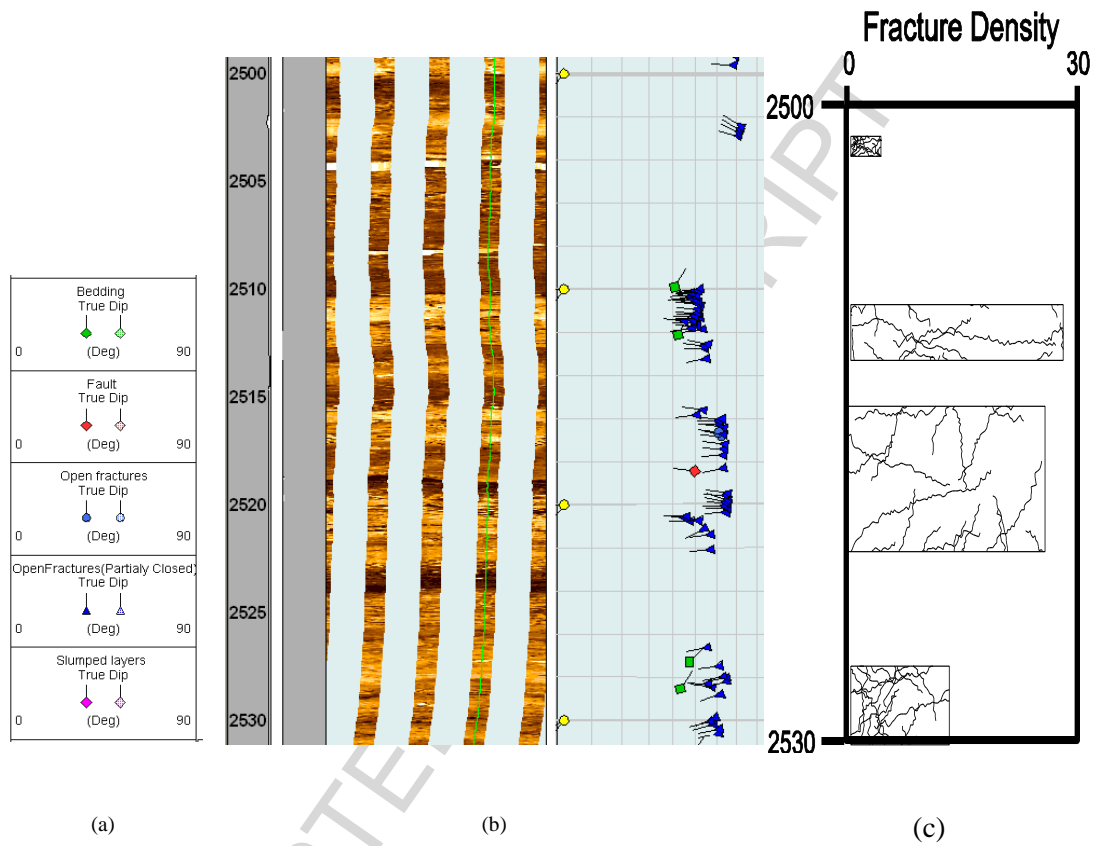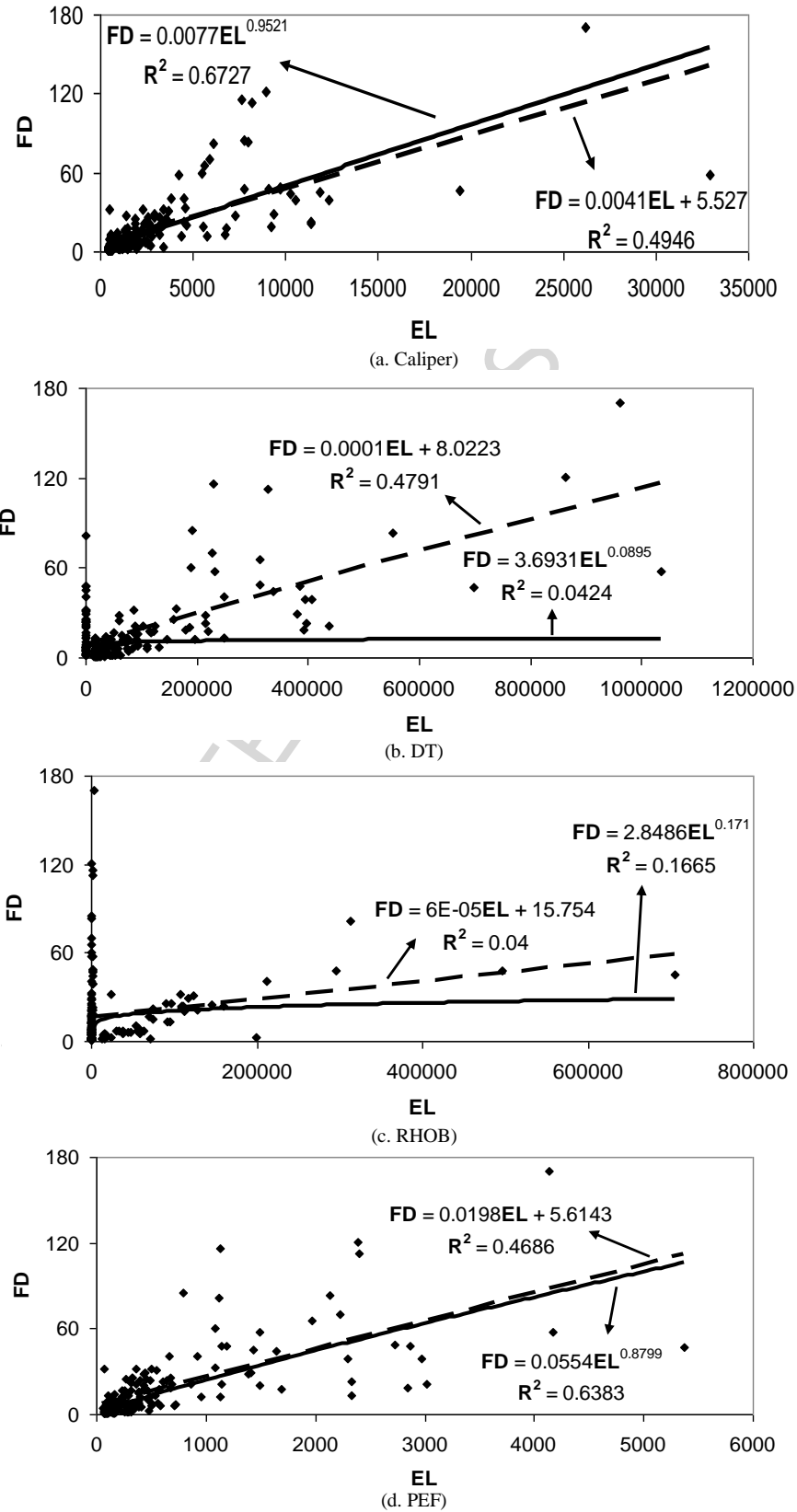Fig. 5

(a. Caliper)

(b. DT)

(c. RHOB)

(d. PEF)

Fig. 6

(a. Caliper)

$FD = 0.0051NEL^{1.0014}$
$R^2 = 0.7355$

(b. DT)

$FD = 0.0002NEL^{1.0014}$
$R^2 = 0.7355$

(c. RHOB)

$FD = 0.0005NEL^{1.0014}$
$R^2 = 0.7355$

(d. PEF)

$FD = 0.0254NEL^{1.0014}$
$R^2 = 0.7355$

14

Fig. 7

Fig. 8

140

FD

70

0

0   2000   4000   6000   8000   10000 12000 14000

FD = 0.0022**NEL**$^{1.1503}$
R^2 = 0.8408

NEL

(a)

180

FD

120

60

0

0   10000   20000   30000

FD = 0.0095**NEL**$^{0.8756}$
R^2 = 0.7368

NEL

(b)

16
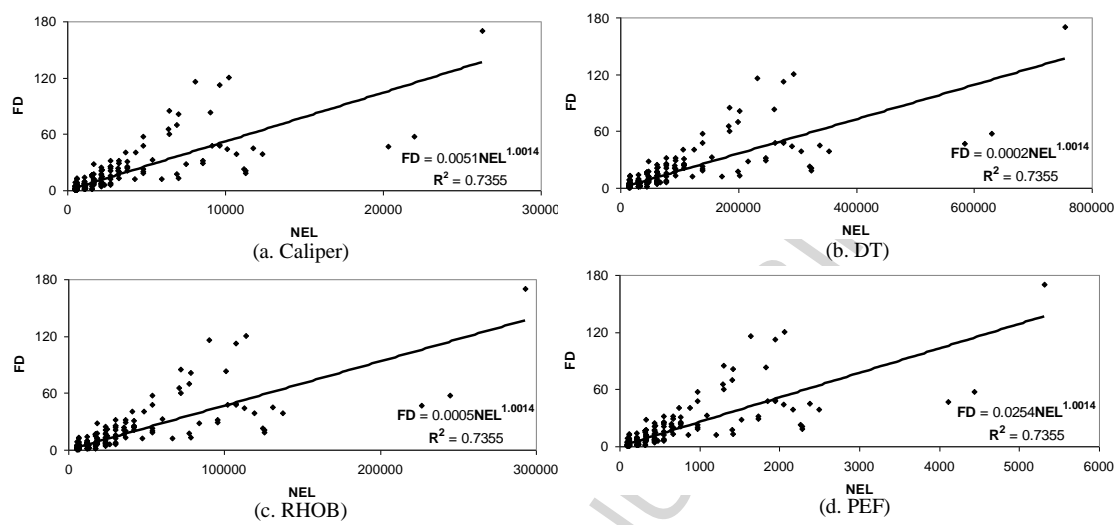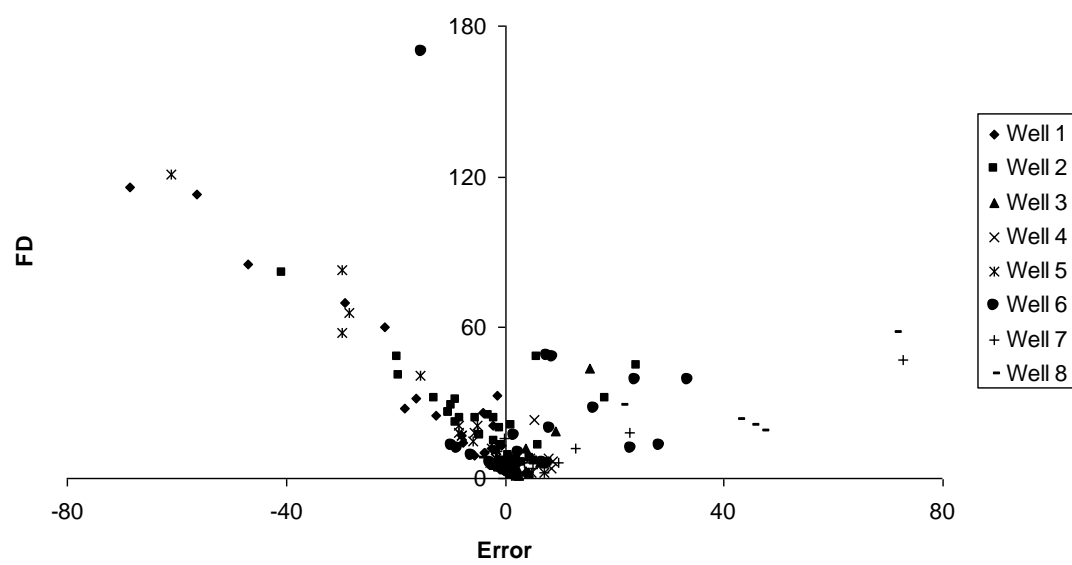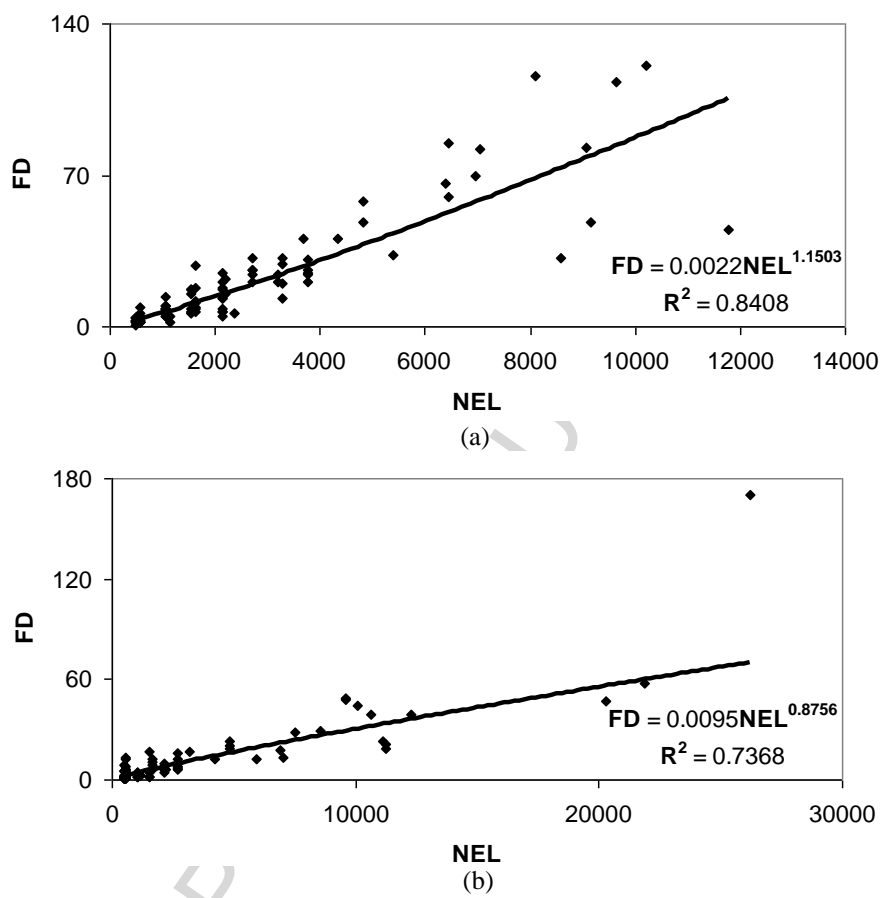
Fig. 9
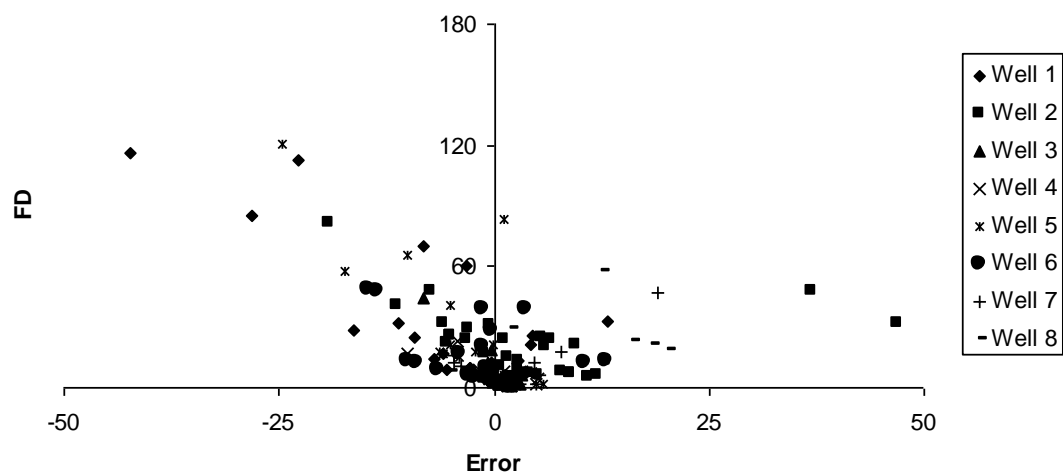
Table 1

Well / PL	1	2	3	4	5	6	7	8
Caliper	0.94	0.81	0.98	0.60	0.97	0.89	0.92	0.95
Uranium	0.70	0.44	0.21		0.54			0.96
CGR	0.66	0.36	0.31	0.49	0.79	0.43	0.05	0.32
SGR	0.77	0.54	0.30		0.64	0.90	0.87	0.97
RT	0.11			0.00	0.05	0.11	0.75	
DT	0.89	0.81	0.98	0.75	0.94	0.91	0.91	0.95
RHOB	0.89	0.78	0.99	0.51	0.96	0.89	0.92	0.88
PEF	0.79	0.76	0.97	0.42	0.94	0.70	0.89	0.73
NPHI	0.16	0.32	0.74		0.71	0.76	0.46	0.92

Table 2

Wells	1	2	3	4	5	6	7	8	Group of wells		
									All	1, 2 and 5	3, 4, 6, 7 and 8
Mean of FD per unit thickness	0.79	0.53	0.30	0.32	0.79	0.39	0.25	0.21	0.48	0.67	0.31